

NEW VIEWS OF SILICIC VOLCANISM ON THE MOON. B. L. Jolliff¹, J. D. Stopar², S. J. Lawrence², M. S. Robinson², and B. R. Hawke³ ¹Department of Earth & Planetary Sciences, Washington University, St. Louis, MO 63130; ²School of Earth and Space Exploration, Arizona State University, Tempe, AZ 85287; ³Hawaii Institute of Geophysics and Planetology, University of Hawaii, Honolulu, Hawaii 96822 (blj@wustl.edu)

Introduction: Spectral “Red Spots” on the Moon have been known for many years [1,2,3]. Some of these spots correspond to domes that are thought to be volcanic in origin. Relatively steep topographic slopes, coupled with other morphologic and compositional evidence indicate that these features are occurrences of silicic or “felsic” volcanism, e.g., rhyolite [3,4,5].

Data collected by remote sensing missions of the past two decades have produced a body of evidence to suggest that large-scale occurrences of felsic rocks exist on the Moon, perhaps the same rock types that are present only as small bits and pieces of breccia clasts and regolith rock fragments in the Apollo collections. A key set of evidence came from the Lunar Prospector (LP) gamma-ray spectrometer (GRS) [6], which revealed substantial concentrations of naturally radioactive thorium (Th), coupled with analyses of felsic Apollo samples that showed strong Th enrichment to be a compositional signature of such rocks [7,8]. Thorium “anomalies” or “hot spots” were identified and correlated to several of the “red spots” [3,6], as well as to ejecta from several nearside impact craters such as Aristarchus (42 km), Aristillus (55 km, and possibly Mairan (40 km), as well as Oresme V (51 km) on the far side. The GRS had a broad spatial response function, over a hundred km, thus correlations to specific small-scale geologic surface units requires caution and spatial deconvolution.

Nevertheless, the global Th map produced by the LP team showed clearly where the major hot spots occur, and it showed several new ones, most notably the Th hot spot that became known as the Compton-Belkovich site [9]. Although Clementine data showed that a relatively high albedo feature might occur at the center of this hot spot [10], it was the high-resolution Lunar Reconnaissance Orbiter Camera (LROC) Narrow Angle Camera (NAC) images that revealed clear evidence of a volcanic terrain at the center of the anomaly [11]. Moreover, the LRO Diviner instrument, whose spectra include three bands in the region of the Christiansen Feature (CF) (~8 microns), shows direct evidence for silica enrichment at this site, corresponding to morphologies and Th concentrations [12,13]. The evidence for multi-km-scale silicic magmatism and volcanism on the Moon at the Compton-Belkovich site and other sites is now firm.

Morphologies and Spatial Scales: Figure 1 compares the topographic and morphologic expression of several of the silicic volcanic complexes, Gruithuisen and Mairan domes, and the Compton-Belkovich (C-B)

and Hansteen-Alpha (H-A) volcanic complexes, using digital terrain models (DTMs) derived from LROC Wide Angle Camera (WAC) images. The diversity of morphologies among these occurrences is striking. The Gruithuisen domes claim the largest volcanic constructs, with the δ and γ domes each over 10 km across and ~1700-1800 m high [5,14]. The Mairan domes range in size, with the largest volcanic constructs being the “middle” and “T” domes, on order of 5-8 km base widths and at least 800 m of vertical relief, and the T dome has a distinctive summit depression [14,15]. The C-B volcanic complex has both large and small volcanic constructs. The α dome is the largest, having a base width of ~6 km and vertical relief of ~800 m [11,14]. The overall complex is a broad dome, ~25×35 km across, with irregular depressions [11]. The H-A complex is a rough-textured triangular mound some 25 km on a side, the margins of which stand ~700 m above the surrounding mare surface and exhibit average slopes of 16-18° [16]. The summit of the arrowhead is ~1 km above the regional mare surface.

Each of these volcanic constructs has regions with relatively steep slopes, ranging from 12° to about 25°, although some of the small topographic features seen in NAC-derived DTMs at H-A and C-B are little more than low-relief circular bulges (e.g., 200-800 m across). In the C-B example, these small bulges also feature distinctive, dense boulder populations [17]. The features with high slopes have been interpreted to represent volcanic cumulo-domes formed from relatively silicic and viscous lavas [e.g., 5, 11, 14, 15]. The low-relief bulges may represent blister-like extrusions of highly viscous lava [18]. Whether the latter features occur at Gruithuisen and Mairan is unknown because mare basalts embay the large domes and cover any low-relief features that might have existed with them.

Origin: Although we have no direct samples of any of these silicic, Th-enriched volcanic hot spots, we do have in the Apollo sample collections numerous small samples of felsic rocks, variably referred to as granite, felsite, or rhyolite. These materials are especially abundant in samples from Apollo 12, 14, and 15. Apollo 12 samples contain an especially diverse set of these materials, including the largest granitic sample, 12013, which is actually a granitic breccia containing two lithologies, granitic material and a mafic, KREEP-rich phase [18].

Arguments can be made for an origin of the granitic phase by silicate-liquid immiscibility during fractionation of KREEP-rich parent magmas, but it

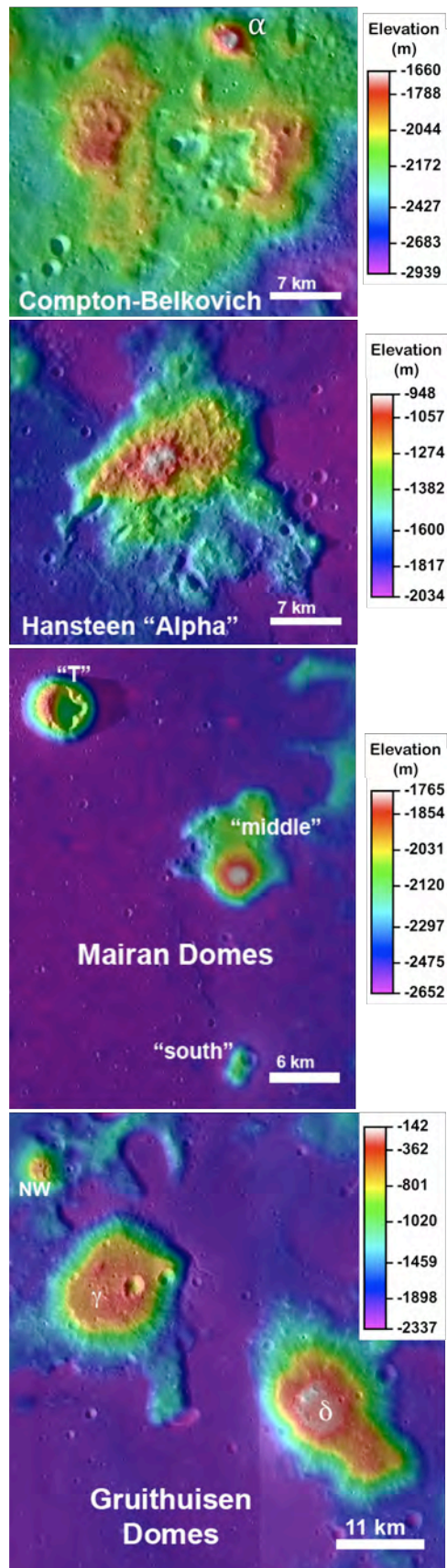


Figure 1. Silicic Volcanic Domes and Complexes; colors represent topography (derived from LRO WAC GLD100 [21]).

remains unclear that this process could or did occur on a large enough scale to source volcanic constructs such as the large domes described above. Perhaps KREEP-rich magmas stalled near the surface and underwent fractional crystallization, producing variably evolved differentiates, some of which were extruded to the surface (e.g., C-B [18]). Among the samples, very high Th concentrations and relatively silica-rich compositions occur in granitic samples and quartz monzogabbro (aka monzodiorite). KREEP basalt itself does not have especially high SiO_2 (<50 wt%) [20], so fractionation is needed to yield the distinctive silica enrichment. High proportions of silica plus K-feldspar in lunar granite could account for the observed SiO_2 enrichment.

Another mechanism that has been proposed is heating of an already KREEP-rich source by basaltic underplating [3], which presumably could produce felsic partial melts directly or could generate KREEP-rich melts that intrude to shallow levels where they further differentiate to produce evolved lavas. So far, among the lunar samples, rocks of intermediate composition between KREEP basalt and rhyolite, such as dacite, are not found. The common process may be the local heating of a KREEP-rich source, which is not difficult to imagine in the central to northern Procellarum region of the Moon where volcanism was extensive, especially in the Aristarchus-Gruithuisen-Mairan triangle. The H-A and C-B occurrences may have involved heating of deeper, KREEP-rich sources, generating KREEP-rich melts that intruded to near the surface before stalling and differentiating. The isolation of C-B favors this interpretation. All of these silicic volcanics have in common that they occur where the crust is relatively thin and the surface is below the lunar mean.

Acknowledgements: We are grateful to the LRO Science & Operations Team and to NASA for support of the LRO Project.

References: [1] Malin M. (1974) *EPSL* **21**, 331. [2] Bruno B. et al., (1991) *PLPS* **21**, 405. [3] Hagerly J. et al. (2006) *JGR* **111**, E06002. [4] Head J. & McCord T. (1978) *Science* **199**, 1433. [5] Head J. & Wilson L. (1999) in *Wkshp on New Views of Moon II*, 23. [6] Lawrence D. et al. (2003) *JGR* **108**, 6-1. [7] Jolliff B. (1998) *JGR* **10**, 916. [8] Seddio S. et al. (2010) *LPS* **41**, #2688. [9] Lawrence D. et al. (1999) *GRL* **26**, 2681-2684. [10] Gillis J. et al. (2002) *LPS* **33**, #1967. [11] Jolliff B. et al. (2011) *Nat. Geosci.* **4**, 566. [12] Glotch T. et al. (2010) *Science* **329**, 1510. [13] Greenhagen B. et al. (2010) *Science* **329**, 1507. [14] Tran T. et al. (2011) *LPS* **42**, #2228. [15] Glotch T. et al. (2011) *GRL* **38**, L2120. [16] Hawke B. et al. (2012) *LPS* **43**, #1754. [17] Accardo N. et al. (2012) *LPS* **43**, #1656. [18] Jolliff B. et al. (2012) *LPS* **43**, #2097. [19] Seddio S. et al. (2011) *LPS* **42**, #2381. [20] Lawrence, D. et al. (2007) *GRL* **34**, L03201. [21] Meyer C. (1977) *Phys. Chem. Earth* **10**, 239. [22] Scholten F. et al. (2012) *JGR* **117**, E00H17.